ARTICLE
Journal of Cellular Biochemistry 113:2290–2295 (2012)

Journal of Cellular Biochemistry

Multi-color Palette of Fluorescent Proteins for Imaging the Tumor Microenvironment of Orthotopic Tumorgraft Mouse Models of Clinical Pancreatic Cancer Specimens

Atsushi Suetsugu,[1,2,3] Matthew Katz,[4] Jason Fleming,[4] Mark Truty,[4] Ryan Thomas,[4] Hisataka Moriwaki,[3] Michael Bouvet,[2] Shigetoyo Saji,[3] and Robert M. Hoffman[1,2*]

[1]*AntiCancer, Inc., San Diego, California*
[2]*Department of Surgery, University of California, San Diego, California*
[3]*Gifu University Graduate School of Medicine, Gifu, Japan*
[4]*Department of Surgical Oncology, MD Anderson Cancer Center, Houston, Texas*

ABSTRACT

Pancreatic-cancer-patient tumor specimens were initially established subcutaneously in NOD/SCID mice immediately after surgery. The patient tumors were then harvested from NOD/SCID mice and passaged orthotopically in transgenic nude mice ubiquitously expressing red fluorescent protein (RFP). The primary patient tumors acquired RFP-expressing stroma. The RFP-expressing stroma included cancer-associated fibroblasts (CAFs) and tumor-associated macrophages (TAMs). Further passage to transgenic nude mice ubiquitously expressing green fluorescent protein (GFP) resulted in tumors that acquired GFP stroma in addition to their RFP stroma, including CAFs and TAMs as well as blood vessels. The RFP stroma persisted in the tumors growing in the GFP mice. Further passage to transgenic nude mice ubiquitously expressing cyan fluorescent protein (CFP) resulted in tumors acquiring CFP stroma in addition to persisting RFP and GFP stroma, including RFP- and GFP-expressing CAFs, TAMs and blood vessels. This model can be used to image progression of patient pancreatic tumors and to visually target stroma as well as cancer cells and to individualize patient therapy. J. Cell. Biochem. 113: 2290–2295, 2012.

KEY WORDS: HUMAN-PATIENT PANCREAS CANCER; IMAGING; TUMOR MICROENVIRONMENT; GFP; RFP; CFP

The athymic, T-cell-deficient, nude mouse has made a very important contribution to cancer research in that it enabled the systemic serial transplantation of human tumors and cell lines [Rygaard and Povlsen, 1969]. Our laboratory pioneered surgical orthotopic implantation (SOI) metastatic nude-mouse models of patient tumor specimens in the early 1990s [Fu et al., 1991, 1992]. These orthotopic mouse models of patient tumors are more patient-like, especially with regard to metastasis, than ectopic subcutaneous models [Rygaard and Povlsen, 1969; Pickard et al., 1975; Giovanella et al., 1978; Nowak et al., 1978; Bailey et al., 1980; Selby et al., 1980; Fiebig et al., 1984, 1987; Sharkey and Fogh, 1984; Steel, 1984; Hwang et al., 2003; Embuscado et al., 2005; Rubio-Viqueira et al., 2006; Garber, 2007; Talmadge et al., 2007; Bertotti et al., 2011]. In our initial development of SOI nude mouse models of patient tumors, we achieved take rates of 65% for colon cancer [Fu et al., 1991] and 100% for pancreatic cancer. Subsequently, the NOD/SCID mouse, was developed [Shultz et al., 1995]. This mouse is deficient in T-, B- and NK cells and allows for higher take rates of patient tumors including 87% for colorectal cancer liver metastasis [Bertotti et al., 2011]. Patient pancreatic tumors have been transplanted to NOD-SCID mice at high frequency [Kim et al., 2009, 2011]. However, these models are limited with regard to studying the tumor microenvironment as well as imaging.

The use of fluorescent proteins for imaging in vivo was pioneered by out laboratory and has been particularly useful to study tumor growth and progression [Hoffman and Yang, 2006a, b; Hoffman, 2005]. With the use of multiple colored fluorescent proteins, we developed imaging of the tumor microenvironment (TME) by color-coding cancer and stromal cells [Yang et al., 2003, 2004, 2007, 2009; Hoffman and Yang, 2006b; Suetsugu et al., 2011, 2012]. With the use of color-coded imaging technology, we have previously demonstrated the essential role of tumor-associated

Grant sponsor: National Cancer Institute; Grant number: CA132971.
*Correspondence to: Robert M. Hoffman, PhD, AntiCancer, Inc., 7917 Ostrow Street, San Diego, CA 92111.
E-mail: all@anticancer.com
Manuscript Received: 11 January 2012; Manuscript Accepted: 3 February 2012
Accepted manuscript online in Wiley Online Library (wileyonlinelibrary.com): 14 February 2012
DOI 10.1002/jcb.24099 • © 2012 Wiley Periodicals, Inc.

host cells in tumor progression and metastasis [Bouvet et al., 2006].

The present study utilizes a pallet of multicolored fluorescent proteins to image the recruitment over time of stromal cells, including cancer-associated fibroblasts (CAFs) and tumor-associated macrophages (TAMs) by pancreatic-cancer-patient tumors grown orthotopically in three types of transgenic nude mice, each expressing a different color fluorescent protein (Yang et al., 2004; Yang et al., 2009; Tran Cao et al., 2009). This study allows for the first time the visualization and demonstration of the persistence of the TME of patient tumors as well and their fluorescence imaging in mouse models.

MATERIALS AND METHODS

SPECIMEN COLLECTION

All patients provided informed consent and samples were procured and the study was conducted under the approval of the Institutional Review Board of the MD Anderson Cancer Center.

GFP, RFP, AND CFP MICE

Transgenic nude C57/B6-GFP, RFP, and CFP mice were obtained from AntiCancer, Inc. (San Diego, CA). These transgenic nude mice express the fluorescent protein gene under the control of the chicken β-actin promoter and cytomegalovirus enhancer. Most of the tissues from these transgenic mice, with the exception of erythrocytes and hair, fluoresce under proper excitation light [Yang et al., 2004; Tran Cao et al., 2009; Yang et al., 2009].

ANIMAL CARE

The transgenic nude mice were bred and maintained in a HEPA-filtered environment at AntiCancer, Inc. with cages, food, water, and bedding sterilized by autoclaving. All surgical procedures and imaging were performed with the animals anesthetized by intramuscular injection of a ketamine mixture. All animal studies were conducted in accordance with the principles of and procedures outlined in the NIH guide for the care and use of laboratory animals under assurance number A3873-1.

ESTABLISHMENT OF TUMORGRAFT MODEL (F1) OF PANCREATIC CANCER PATIENT TUMORS

Pancreas cancer patient tumor tissue was obtained at surgery and cut into 3-mm^3 fragments and transplanted subcutaneously in NOD/SCID mice (Kim et al., 2009, 2011).

ORTHOTOPIC TUMORGRAFT (F2) OF PANCREATIC CANCER PATIENT TUMORS IN TRANSGENIC RFP NUDE MICE

The F1 tumors from NOD/SCID mice were harvested and cut into 3-mm^3 fragments and transplanted orthotopically [Hoffman, 1999] in 6-week-old transgenic nude RFP mice (Yang et al., 2009) (F2 model).

ORTHOTOPIC TUMORGRAFT (F3) OF PANCREATIC CANCER PATIENT TUMORS IN TRANSGENIC GFP NUDE MICE

The F2 tumors were harvested from the RFP nude mice and were cut into 3-mm^3 fragments and transplanted orthotopically [Hoffman, 1999] in 6-week-old transgenic nude GFP mice (Yang et al., 2009) (F3 model).

ORTHOTOPIC TUMORGRAFT (F4) OF PANCREATIC CANCER PATIENT TUMORS IN TRANSGENIC CFP NUDE MICE

The F3 tumors were harvested from the GFP nude mice and cut into 3-mm^3 fragments and transplanted orthotopically [Hoffman, 1999] in 6-week-old transgenic nude CFP mice (Tran Cao et al., 2009) (F4 model).

TUMOR IMAGING

The OV100 variable magnification Small Animal Imaging System [Yamauchi et al., 2006], the FV1000 confocal microscope [Uchugonova et al., 2011], and the MVX10 long-working distance fluorescence dissecting microscope [Kimura et al., 2010], all from Olympus Corp. (Tokyo, Japan), were used in this study.

RESULTS AND DISCUSSION

ENGRAFTMENT OF PATIENT TUMORS (F1) IN NOD/SCID MOUSE

A flow diagram experimental protocols is shown (Fig. 1A). Human pancreatic-cancer patient tumors were initially transplanted subcutaneously in NOD/SCID mice. Tumors were detected by day-30. Tumors were harvested from the NOD/SCID mice.

RFP HOST STROMAL CELLS INFILTRATE ORTHOTOPIC PANCREATIC CANCER TUMORGRAFTS (F2)

The harvested human pancreatic cancer patient tumors from the NOD/SCID mice were transplanted orthotopically in 6-week-old transgenic RFP nude mice (F2 model). After 30 days, tumors were imaged using the OV100 (Fig. 1B). The RFP stromal cells from the RFP host mice formed a capsule around the F2 tumor (Fig. 1B) and infiltrated into the central part of the tumor as well (Fig. 1C). RFP-expressing TAMs could be visualized in the tumor (Fig. 1D).

GFP HOST STROMAL CELLS INFILTRATE THE ORTHOTOPIC PANCREATIC CANCER TUMORGRAFTS TO FORM A TWO-COLOR STROMA MODEL (F3)

The F2 tumor was harvested at day-30, cut into 3-mm^3 pieces, and transplanted orthotopically in 6-week-old transgenic GFP nude mice (F3 model). After 30 days, tumors were imaged with the OV100 (Fig. 1E). The F2 tumor spread on the host GFP pancreas (Fig. 1F). After 56 days, tumors were removed from the GFP nude mice. The human pancreatic-cancer-patient tumors contained both RFP and GFP stromal cells (Fig. 1G). The RFP stromal cells still persisted after passage in the F3 tumorgraft. Under confocal microscopy with the FV1000, RFP and GFP stromal cells were clearly visualized in the tumor (Fig. 1H). GFP and RFP CAFs and TAMs were visualized including in the central part of the tumor (Fig. 1H–J).

CFP HOST STROMAL CELLS INFILTRATE ORTHOTOPIC PANCREATIC CANCER TUMORGRAFTS TO FORM A THREE-COLOR STROMA MODEL (F4)

F3 tumors were harvested at day-56 and transplanted orthotopically in 6-week-old nude CFP mice (F4 model). After 30 days, F4 tumors were observed with the MVX10 long-working-distance fluorescence

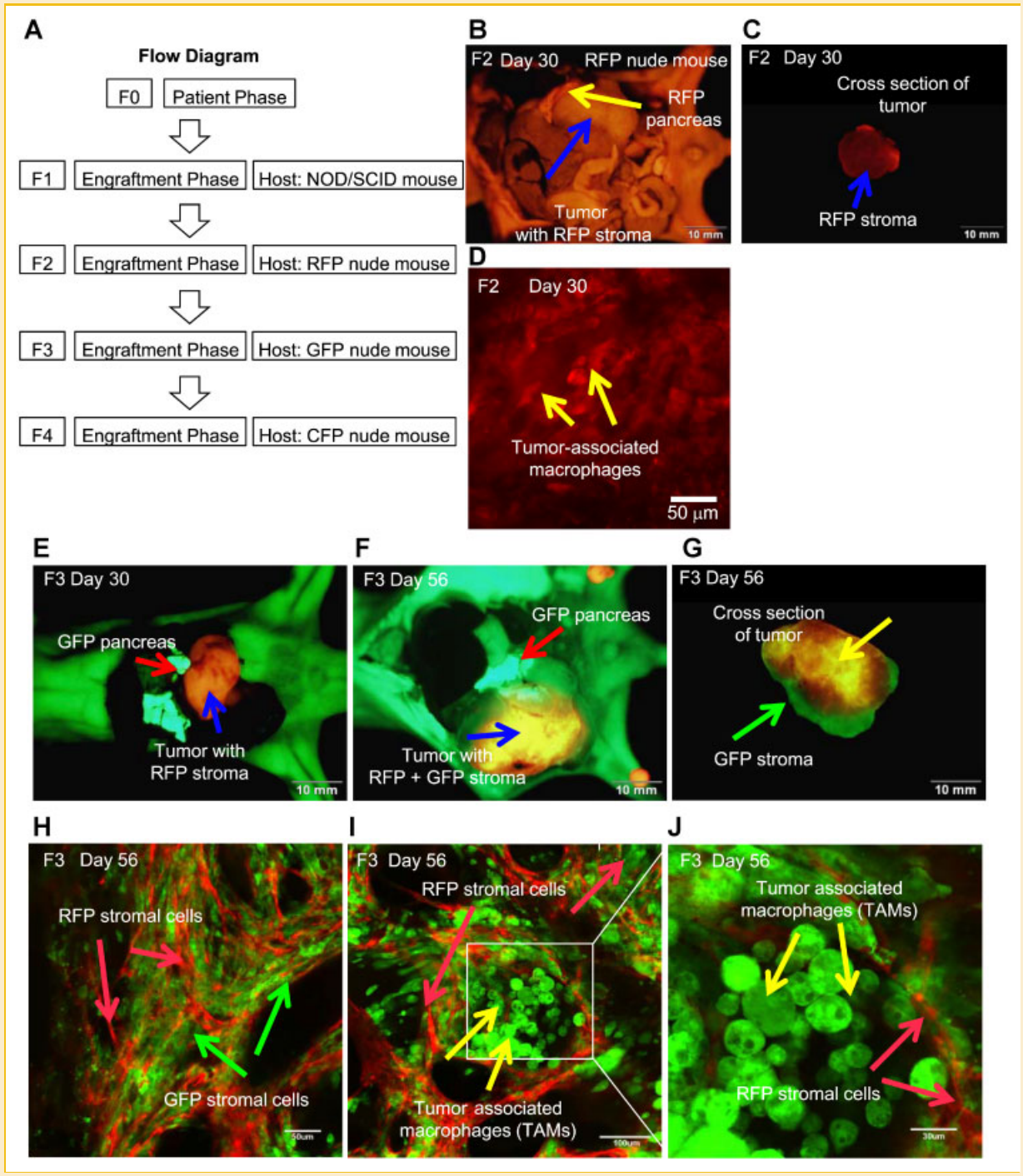

Fig. 1. A: Flow diagram of the experimental protocol. B: Orthotopic tumorgraft model (F2) of human pancreatic-cancer-patient tumor transplanted to RFP transgenic nude mouse. Yellow arrow indicates host RFP nude mouse pancreas. Blue arrow indicates tumor with infiltrating RFP stroma (Bar = 10 mm). Image taken with the Olympus OV100. C: Human pancreatic tumor excised from RFP nude mouse with RFP stroma. The image is of a cross-section of the tumor. Blue arrow indicates RFP stroma (Bar = 10 mm). Image taken with the Olympus OV100. D: Visualization of RFP tumor-associated macrophages (TAMs) in the human pancreatic cancer patient tumor (F2). High-magnification image taken with the Olympus FV1000 confocal microscope. Yellow arrows indicate RFP TAMs (Bar = 50 μm). E: Orthotopic tumorgraft model (F3) of human pancreatic-cancer-patient tumor growing in transgenic GFP nude mice for 30 days. Red arrow indicates host GFP nude mouse pancreas. Blue arrow indicates human pancreatic tumor with RFP stroma (Bar = 10 mm). Image taken with the Olympus OV100. F: Pancreatic tumor growing in GFP-host model for 56 days. Red arrow indicates host GFP nude mouse pancreas. Blue arrow indicates human pancreatic tumor with RFP + GFP stroma (Bar = 10 mm). Image taken with the Olympus OV100. G: Excised tumor with RFP and GFP stroma. The image is of a cross-section of the tumor. Yellow arrow indicates RFP stroma. Green arrow indicates GFP stroma (Bar = 10 mm). Image taken with the Olympus FV1000. H: Human pancreatic-cancer-patient tumor (F3) with RFP and GFP stromal cells. Image was taken with the Olympus FV1000. Green arrows indicate GFP stromal cells from GFP mouse. Red arrows indicate RFP stromal cells from RFP mouse. (Bar = 50 μm) I: Human pancreatic-cancer-patient tumor with RFP stromal cells and GFP TAMs. (Bar = 100 μm). Image taken with the Olympus FV1000. J: High magnification image of (I). RFP stromal cells and GFP-TAMs are readily observed. (Bar = 30 μm). Image taken with the Olympus FV1000.

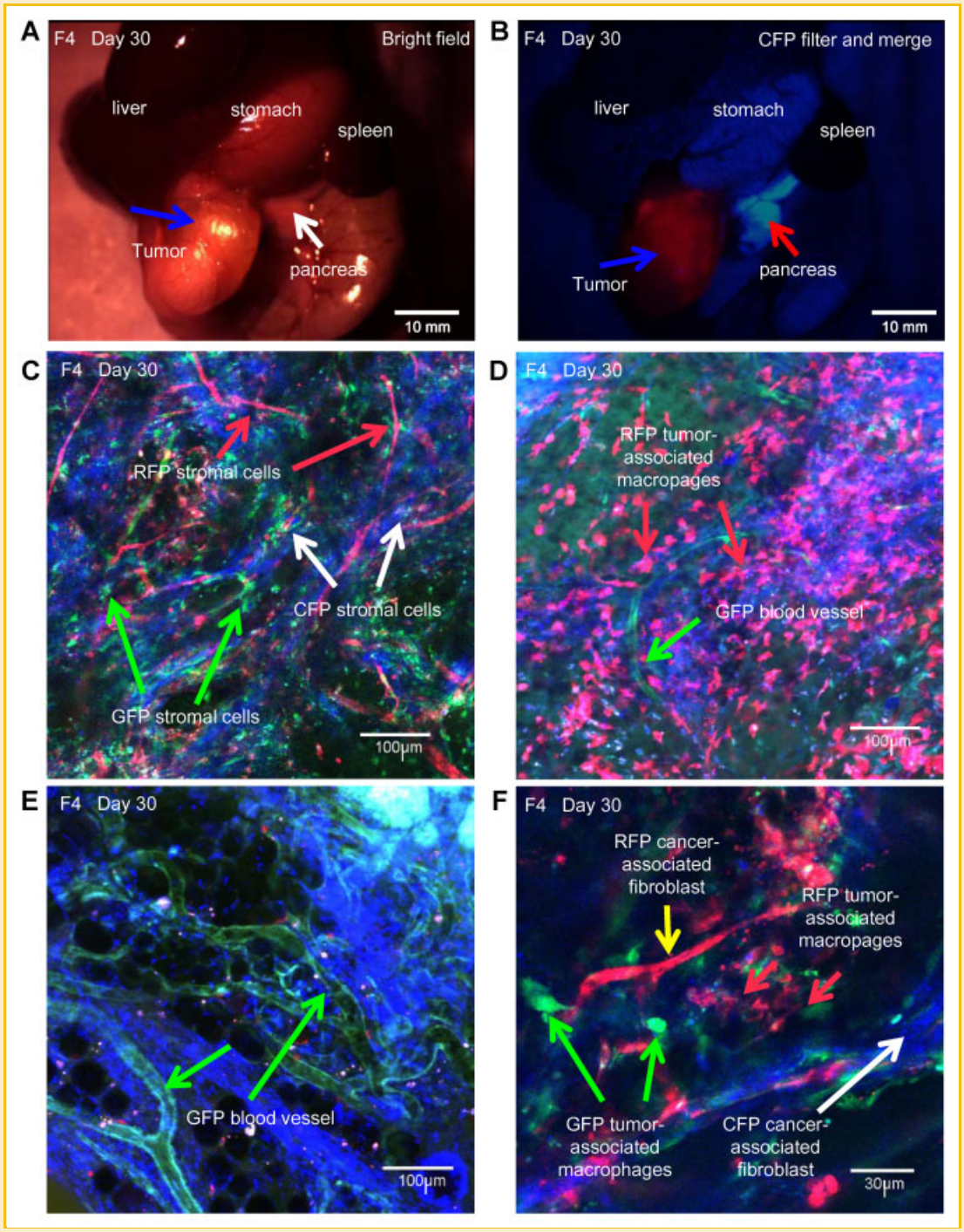

Fig. 2. A: Human pancreatic-cancer-patient tumor growing in CFP-host (F4). White arrow indicates host CFP nude mouse pancreas. Blue arrow indicates tumor. Image was taken with the Olympus MVX10 microscope (Bar = 10 mm). B: Human pancreatic-cancer-patient tumor (F4) (blue arrow) with RFP, GFP, and CFP stromal cells. Red arrow indicates CFP pancreas. Image was taken with the MVX10 (Bar = 10 mm). C: RFP, GFP, and CFP stromal cells were observed. Red arrow indicates RFP stromal cells. Green arrows indicate GFP stromal cells. White arrows indicate CFP stromal cells (Bar = 100 μm). Image taken with the FV1000 confocal microscope. D: RFP TAMs (red arrow) and GFP blood vessel (green arrow) were observed in the F4 tumor (Bar = 100 μm). Image taken with the Olympus FV1000 confocal microscope. E: GFP blood vessels (green arrows) in the F4 tumor. (Bar = 100 μm). Image was taken with the FV1000 confocal microscope. F: RFP CAFs (yellow arrow) and GFP TAMs (green arrows) in the F4 tumor. White arrow indicates CFP CAFs. (Bar = 30 μm). Image was taken with the FV1000 confocal microscope.

microscope (Fig. 2A,B). The excised F4 tumor was also observed with the FV1000 confocal microscope (Fig. 2C–F). RFP-, GFP-, and CFP-expressing stromal cells were observed in the human pancreatic-cancer patient tumor (Fig. 2C). The RFP stroma persisted after two passages and GFP stroma persisted after one passage in the F4 model in CFP mice. RFP TAMs and CAFs (Fig. 2D,F) and GFP blood vessels (Fig. 2D,E) still persisted in the human pancreatic-cancer patient tumor after 2 and 1 passages, respectively (Fig. 2F).

We have thus demonstrated a new mouse model of cancer-patient tumors, whereby stromal elements can be imaged using a pallet of multi-color fluorescent proteins. The fluorescent stroma persisted for at least two passages in the tumors growing in the transgenic mice, indicating the intimacy of cancer cells and stroma. The survival of stroma after transplantation was previously suggested [Duda et al., 2004]. The results of the present study demonstrate the serial transplantability of stroma. For example from the RFP mice, TAMs and CAFs persisted from F2 to F4, suggesting they may be proliferating along with the cancer cells in the tumor. From the GFP mice, TAMs and CAFs and blood vessels were found in the tumor and persisted to F4. The CFP mice contributed mostly CAFs to the tumor. The fluorescent stroma allow the entire tumor to be imaged as well. Both standard and novel cancer- and stroma-targeting agents can be tested in this model and can be used for individualized therapy of cancer patients.

The new models described in this report offer many opportunities. For example, cell lines can be established from the tumors with fluorescent stroma and the role of stroma in cell line establishment can be imaged longitudinally.

The stromal cells of each fluorescent color can be isolated by fluorescence-activated cell sorting (FACS) to further characterize them.

Since the stroma carry genes for fluorescent proteins, it may be possible to observe gene transfer from stromal cells to the cancer cells. We have previously taken advantage of differential fluorescent protein expression in cancer cells to demonstrate gene transfer between cancer cells in vivo [Glinsky et al., 2006; Tome et al., 2009].

It should also be possible to determine if some of the fluorescent stromal cells are derived from tissue-specific stem cells or mesenchymal stem cells.

One of the most exciting opportunities directly inspired by observations in the current study and enabled by the availability of the color-coded panel of hosts, would be the analysis of the role, requirements, and contribution of host stroma to metastatic initiation and progression.

REFERENCES

Bailey MJ, Gazet JC, Peckham MJ. 1980. Human breast-cancer xenografts in immune-suppressed mice. Br J Cancer 42:524–529.

Bertotti A, Migliardi G, Galimi F, Sassi F, Torti D, Isella C, Corà D, Di Nicolantonio F, Buscarino M, Petti C, Ribero D, Russolillo N, Muratore A, Massucco P, Pisacane A, Molinaro L, Valtorta E, Sartore-Bianchi A, Risio M, Capussotti L, Gambacorta M, Siena S, Medico E, Sapino A, Marsoni S, Comoglio PM, Bardelli A, Trusolino L. 2011. A molecularly annotated platform of patient-derived xenografts (''Xenopatients'') identifies HER2 as an effective therapeutic target in cetuximab-resistant colorectal cancer. Cancer Disc 1:508–523.

Bouvet M, Tsuji K, Yang M, Jiang P, Moossa AR, Hoffman RM. 2006. In vivo color-coded imaging of the interaction of colon cancer cells and splenocytes in the formation of liver metastases. Cancer Res 66:11293–11297.

Duda DG, Fukumura D, Munn LL, Booth MF, Brown EB, Huang P, Seed B, Jain RK. 2004. Differential transplantability of tumor-associated stromal cells. Cancer Res 64:5920–5924.

Embuscado EE, Laheru D, Ricci F, Yun KJ, de Boom Witzel S, Seigel A, Flickinger K, Hidalgo M, Bova GS, Iacobuzio-Donahue CA. 2005. Immortalizing the complexity of cancer metastasis: Genetic features of lethal metastatic pancreatic cancer obtained from rapid autopsy. Cancer Biol Ther 4:548–554.

Fiebig HH, Widmer K-H, Fiedler L, Wittekind C, Löhr GW. 1984. Development and characterization of 51 human tumor models for large bowel, stomach and esophageal cancer. Dig Surg 1:225–235.

Fiebig HH, Schmid JR, Bieser W, Henss H, Löhr GW. 1987. Colony assay with human tumor xenografts, murine tumors and human bone marrow. Potential for anticancer drug development. Eur J Cancer Clin Oncol 23:937–948.

Fu X, Besterman JM, Monosov A, Hoffman RM. 1991. Models of human metastatic colon cancer in nude mice orthotopically constructed by using histologically intact patient specimens. Proc Natl Acad Sci USA 88:9345–9349.

Fu X, Guadagni F, Hoffman RM. 1992. A metastatic nude-mouse model of human pancreatic cancer constructed orthotopically with histologically intact patient specimens. Proc Natl Acad Sci USA 89:5645–5649.

Garber K. 2007. Personal mouse colonies give hope for pancreatic cancer patients. J Natl Cancer Inst 99:105–107.

Giovanella BC, Stehlin JS Jr, Williams LJ Jr, Lee SS, Shepard RC. 1978. Heterotransplantation of human cancers into nude mice: A model system for human cancer chemotherapy. Cancer 42:2269–2281.

Glinsky GV, Glinskii AB, Berezovskaya O, Smith BA, Jiang P, Li X-M, Yang M, Hoffman RM. 2006. Dual-color-coded imaging of viable circulating prostate carcinoma cells reveals genetic exchange between tumor cells in vivo, contributing to highly metastatic phenotypes. Cell Cycle 5:191–197.

Hoffman RM. 1999. Orthotopic metastatic mouse models for anticancer drug discovery and evaluation: A bridge to the clinic. Investig New Drugs 17:343–359.

Hoffman RM. 2005. The multiple uses of fluorescent proteins to visualize cancer in vivo. Nat Rev Cancer 5:796–806.

Hoffman RM, Yang M. 2006a. Subcellular imaging in the live mouse. Nat Protoc 1:775–782.

Hoffman RM, Yang M. 2006b. Color-coded fluorescence imaging of tumor-host interactions. Nat Protoc 1:928–935.

Hwang RF, Yokoi K, Bucana CD, Tsan R, Killion JJ, Evans DB, Fidler IJ. 2003. Inhibition of platelet-derived growth factor receptor phosphorylation by STI571 (Gleevec) reduces growth and metastasis of human pancreatic carcinoma in an orthotopic nude mouse model. Clin Cancer Res 9:6534–6544.

Kim MP, Evans DB, Wang H, Abbruzzese JL, Fleming JB, Gallick GE. 2009. Generation of orthotopic and heterotopic human pancreatic cancer xenografts in immunodeficient mice. Nat Protol 4:1670–1680.

Kim MP, Truty MJ, Choi W, Kang Y, Chopin-Lally X, Gallick GE, Wang H, McConkey DJ, Hwang R, Logsdon C, Abbruzzesse J, Fleming JB. 2011. Molecular profiling of direct xenograft tumors established from human pancreatic adenocarcinoma after neoadjuvant therapy. Ann Surg Oncol [Epub ahead of print]. DOI: 10.1245/s10434-011-1839-4

Kimura H, Momiyama M, Tomita K, Tsuchiya H, Hoffman RM. 2010. Long-working-distance fluorescence microscope with high-numerical-aperture objectives for variable-magnification imaging in live mice from macro- to subcellular. J Biomed Optics 15:066029.

Nowak K, Peckham MJ, Steel GG. 1978. Variation in response of xenografts of colo-rectal carcinoma to chemotherapy. Br J Cancer 37:576–584.

Pickard RG, Cobb LM, Steel GG. 1975. The growth kinetics of xenografts of human colorectal tumours in immune deprived mice. Br J Cancer 31: 36–45.

Rubio-Viqueira B, Jimeno A, Cusatis G, Zhang X, Iacobuzio-Donahue C, Karikari C, Shi C, Danenberg K, Danenberg PV, Kuramochi H, Tanaka K, Singh S, Salimi-Moosavi H, Bouraoud N, Amador ML, Altiok S, Kulesza P, Yeo C, Messersmith W, Eshleman J, Hruban RH, Maitra A, Hidalgo M. 2006. An in vivo platform for translational drug development in pancreatic cancer. Clin Cancer Res 12:4652–4661.

Rygaard J, Povlsen CO. 1969. Heterotransplantation of a human malignant tumour to "Nude" mice. Acta Pathol Microbiol Scand 77:758–760.

Selby PJ, Courtenay VD, McElwain TJ, Peckham MJ, Steel GG. 1980. Colony growth and clonogenic cell survival in human melanoma xenografts treated with chemotherapy. Br J Cancer. 42:438–447.

Sharkey FE, Fogh J. 1984. Consideration in the use of nude mice for cancer research. Cancer Metastasis Rev 3:341–360.

Shultz LD, Schweitzer PA, Christianson SW, Gott B, Schweitzer IB, Tennent B, McKenna S, Mobraaten L, Rajan TV, Greiner DL, et al. 1995. Multiple defects in innate and adaptive immunologic function in NOD/LtSz-scid mice. J Immunol 154:180–191.

Steel GG. 1984. Therapeutic response of human tumour xenografts in immune-suppressed mice. In: Sordat B, editor. Immune-deficient animals, 4th Int. Workshop on Immune-Deficient Animals in Exp. Res. (Chexbres, Oct. 31–Nov 3, 1982). Switzerland: Karger. pp 395–404.

Suetsugu A, Osawa, Y, Nagaki M, Saji S, Moriwaki H, Bouvet M, Hoffman RM. 2011. Imaging the recruitment of cancer-associated fibroblasts by liver-metastatic colon cancer. J Cell Biochem 112:949–953.

Suetsugu A, Hassanein MK, Reynoso J, Osawa Y, Nagaki M, Moriwaki H, Saji S, Bouvet M, Hoffman RM. 2012. The cyan fluorescent protein nude mouse as a host for multicolor-coded imaging models of primary and metastatic tumor microenvironments. Anticancer Res 32:31–38.

Talmadge JE, Singh RK, Fidler IJ, Raz A. 2007. Murine models to evaluate novel and conventional therapeutic strategies for cancer. Am J Pathol 170:793–804.

Tome Y, Tsuchiya H, Hayashi K, Yamauchi K, Sugimoto N, Kanaya F, Tomita K, Hoffman RM. 2009. In vivo gene transfer between interacting human osteosarcoma cell lines is associated with acquisition of enhanced metastatic potential. J Cell Biochem 108:362–367.

Tran Cao HS, Kimura H, Kaushal S, Snyder CS, Reynoso J, Hoffman RM, Bouvet M. 2009. The cyan fluorescent protein (CFP) transgenic mouse as a model for imaging pancreatic exocrine cells. J Pancreas 10:152–156.

Uchugonova A, Duong J, Zhang N, König K, Hoffman RM. 2011. The bulge area is the origin of nestin-expressing pluripotent stem cells of the hair follicle. J Cell Biochem 112:2046–2050.

Yamauchi K, Yang M, Jiang P, Xu M, Yamamoto N, Tsuchiya H, Tomita K, Moossa AR, Bouvet M, Hoffman RM. 2006. Development of real-time subcellular dynamic multicolor imaging of cancer-cell trafficking in live mice with a variable-magnification whole-mouse imaging system. Cancer Res 66:4208–4214.

Yang M, Li L, Jiang P, Moossa AR, Penman S, Hoffman RM. 2003. Dual-color fluorescence imaging distinguishes tumor cells from induced host angiogenic vessels and stromal cells. Proc Natl Acad Sci USA 100:14259–14262.

Yang M, Reynoso J, Jiang P, Li L, Moossa AR, Hoffman RM. 2004. Transgenic nude mouse with ubiquitous green fluorescent protein expression as a host for human tumors. Cancer Res 64:8651–8656.

Yang M, Jiang P, Hoffman RM. 2007. Whole-body subcellular multicolor imaging of tumor-host interaction and drug response in real time. Cancer Res 67:5195–5200.

Yang M, Reynoso J, Bouvet M, Hoffman RM. 2009. A transgenic red fluorescent protein-expressing nude mouse for color-coded imaging of the tumor microenvironment. J Cell Biochem 106:279–284.